

Interaction Possibilities of Bonded and Loose Particles in LS-DYNA®

Nils Karajan¹, Zhidong Han², Hailong Ten², Jason Wang²

¹ DYNAmore GmbH, Industriestraße 2, 70569 Stuttgart, Germany
eMail: nils.karajan@dynamore.de, Web: <http://www.dynamore.de>

² Livermore Software Technology Corp. (LSTC), 7374 Las Positas Road, Livermore, CA 94551, USA
eMail: support@lstc.com, Web: <http://www.lstc.com>

1 Introduction

The goal of this presentation is to outline the current development status of LS-DYNA® with respect to simulations using the discrete-element method (DEM), which is based on Cundall & Strack [1]. Starting with assemblies of loose discrete spherical particles, different types of granular media can be discretized to predict their behavior, for instance, during mixing processes, storage and discharge in silos or transportation on belts. Following this, the interaction of the discrete particles with themselves as well as their surrounding deformable or rigid structures can be taken into account. Herein, friction coefficients as well as spring and damping constants can be defined in normal and tangential direction. Wet particles can be estimated with the aid of a capillary force model. Even though the geometric shape of the particles is always spherical, a certain roughness of the grains can be achieved by introducing a rolling friction or by defining clustered particles using bonds.

Moreover, with the introduction of bonded particles, linear-elastic solid material behavior can be modeled. Herein, the mechanical behavior of the bonds may either be prescribed manually or computed internally by LS-DYNA in an automated fashion using the elastic constants given in a material card. With the definition of a fracture energy release rate of the bonds, fracture mechanics of brittle materials can be studied. Herein, the number of bonds of a particle to the neighboring particles can be defined with a bond radius. Note that the breakage of single bonds can be interpreted as micro cracks that eventually evolve to macro cracks.

This presentation will give an overview of the involved material cards and provides information on how the cards are used. For a better understanding of the involved parameters, simple examples will be presented addressing particle-particle as well as particle-structure interaction.

2 The Discrete-Element Method in LS-DYNA

In LS-DYNA, the DEM is realized using rigid spherical particles, while interactions with other rigid or deformable structures are accomplished using penalty-based contact algorithms. Note that the DEM computes the motion of each spherical particle using Newton's law of motion and thus, each particle may have three displacements and three rotations as degrees of freedom. Following this, stress and strain fields are not directly available using the DEM. This is also the difference to other mesh-free methods like Smoothed-Particle Hydrodynamics (SPH) or Element-Free Galerkin (EFG), which are used as discretization schemes for the fundamental continuum-mechanical balance equations.

2.1 Particle Definition

All particles need to be combined in a `*PART` using a "blank" `*SECTION_SOLID`. The definition of the particles is done using the card `*ELEMENT_DISCRETE_SPHERE_OPTION`, which requires the initial coordinate of each sphere to be given via the node ID of `*NODE` as well as its respective radius. The missing values for mass M and inertia I need to be computed and prescribed for each particle using

$$M = V\rho = \frac{4}{3}\pi r^3\rho \quad \text{and} \quad I = \frac{2}{5}Mr^2 = \frac{8}{15}\pi r^5\rho. \quad (1)$$

If the option ***ELEMENT_DISCRETE_SPHERE_VOLUME** is used, the values for mass and inertia need to be prescribed using a normalized density of $\rho = 1$, whereas the real material density of the particles is taken from ***MAT_ELASTIC** to scale the prescribed values of mass and inertia internally in LS-DYNA.

```

*PART
$#-----1-----2-----3-----4-----5-----6-----7-----8
$#  TITLE
Spherical Particles
$#  PID      SECID      MID      EOSID      HGID      GRAV      ADPOPT      TMID
    42        42        42        0          0          0          0          0
*SECTION SOLID
$#  SECID      ELFORM      AET
    42          0          0
*MAT_ELASTIC
$#  MID      RO      E      PR      N      COUPLE      M      ALIAS
    42  7.830e03  2.070e11  0.3
*ELEMENT_DISCRETE_SPHERE_VOLUME
$#  NID      PID      MASS      INERTIA      RADII
    30001     42  570.2710  6036.748     5.14
    30002     42  399.0092  3328.938     4.57
    30003     42  139.1240  575.004     3.21
*NODE
$#-----1-----2-----3-----4-----5-----6
$#  NID      X      Y      Z      TC      RC
    30001     -29.00  -26.8  8.7  0  0
    30002     -21.00  -24.8  18.2  0  0
    30003     -27.00  -14.7  21.2  0  0

```

2.2 Particle-Particle Interaction

The penalty-based particle-particle interaction is specified using ***CONTROL_DISCRETE_ELEMENT**, which provides the possibility to define normal and tangential stiffness and damping coefficients, static friction and rolling friction coefficients, as well as a liquid surface tension to account for capillary forces between wet particles, cf. Figure 1a).

```

*CONTROL_DISCRETE_ELEMENT
$#-----1-----2-----3-----4-----5-----6-----7-----8
$#  NDAMP      TDAMP      Fric      FricR      NormK      ShearK      CAP      MXNSC
    0.700      0.400      0.41      0.001      0.01      0.0029      0  0
$#  Gamma      CAPVOL      CAPANG
    26.4      0.66      10.0

```

Following this, three different collision states can be distinguished, which depend on the interaction distance, which is indicated in Figure 1b), viz.:

$$d_{\text{int}} = r_1 + r_2 - |\mathbf{x}_1 - \mathbf{x}_2| . \quad (2)$$

The first case describes the mechanical contact situation, where penetrations may occur due to the penalty formulation of the contact. In the case of wet particles, the liquid surface tension of the wetting agent may lead to so-called liquid bridges that cause an attracting force between adjacent particles.

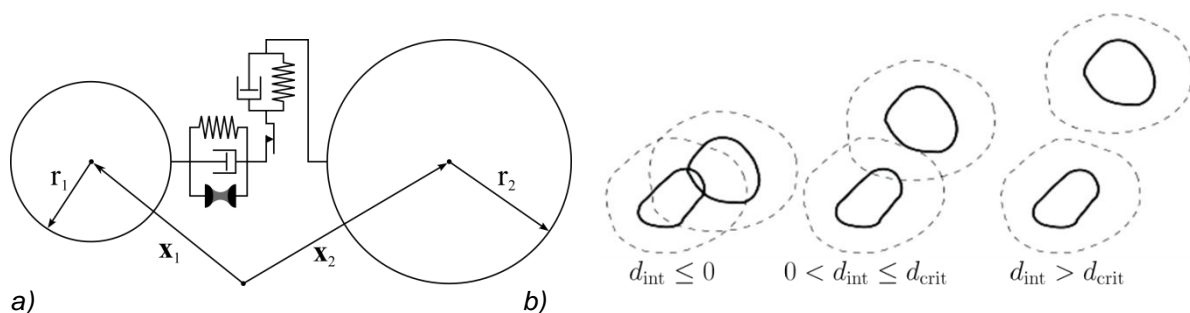


Fig. 1: a) Penalty-based particle-particle interaction in LS-DYNA and b) possible collision states

Subsequently, this introduces another collision state depending on a rupture distance d_{crit} of the liquid bridge, i. e., the distance where the liquid bridge brakes and the adjacent particles are not interacting anymore.

The most important quantity that influences the mechanical penalty-based particle-particle contact is the elastic contribution of the spring elements. Herein, the normal contact force contribution is given by

$$F_n = K_n d_{\text{int}} \quad \text{with} \quad K_n = \begin{cases} \frac{\kappa_1 r_1 \kappa_2 r_2}{\kappa_1 r_1 + \kappa_2 r_2} \text{NormK} & : \text{if NormK} > 0 \\ \text{NormK} & : \text{if NormK} < 0 \end{cases} \quad \text{and} \quad \kappa = \frac{E}{3(1-2\nu)}, \quad (3)$$

where κ_i are the compression moduli that are computed by LS-DYNA using the constants given in ***MAT_ELASTIC**. Thus, if NormK is greater than zero, it is understood as a scale factor and if it is less than zero the normal stiffness can be directly prescribed. Note that the tangential spring constant is given relative to the normal spring constant using $K_t = K_n \text{ShearK}$. Suggested default values for NormK and ShearK are 0.01 and $\frac{2}{7} = 0.2857$, respectively.

The damping behavior of the particle-particle contact is dominated by the damping force, for instance the contribution in normal direction via

$$F_n = D_n \dot{d}_{\text{int}}. \quad (4)$$

Note that the parameters NDAMP and TDAMP define the ratio of the critical damping in the normal and tangential directions, respectively, yielding

$$D_{n/t} = \text{DAMP} \eta_{\text{crit}} = 2.0 \text{DAMP} \sqrt{\frac{m_1 m_2}{m_1 + m_2}} K_{n/t} \quad \text{with} \quad 0 \leq \text{DAMP} \leq 1.0. \quad (5)$$

Figure 2 shows the influence of the normal damping on a particle that is dropped onto another particle from 1m height under gravity loading.

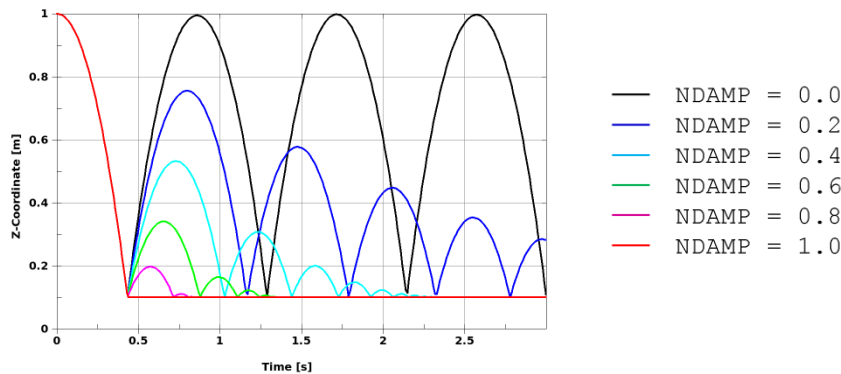


Fig 2: Influence of the normal damping during particle-particle contact resulting from a drop under gravity loading from a height of 1m.

The frictional force component F_{fr} of the mechanical particle-particle contact is based on Coulombs law of dry friction

$$F_{fr} = \mu_{fr} F_n, \quad (6)$$

which depends on the friction coefficient μ_{fr} (Fric) and the sum of all normal forces F_n given in (3) and (4). Note that a vanishing friction coefficient yields a central force system for each particle and thus, LS-DYNA reduces the degrees of freedom (DOF) of each spherical particle to three translations. Moreover, only friction coefficients greater than zero allow tangential friction forces to be induced at the perimeter of a spherical particle and thus, yield a general force system and the need for six DOF per spherical particle in LS-DYNA, i. e., three translations and three rotations.

To account for a certain surface roughness of the spherical particles or even to approximate other particle shapes like polygonal particles, the DEM in LS-DYNA is extended by the introduction of a rolling resistance FricR. Typical values for sand grains lie around FricR = 0.01, depending on the smoothness of the grains.

Finally, capillary forces that occur between wet particles can be switched on in LS-DYNA using CAP = 1, which triggers the need to define the optional parameters for the liquid surface tension Gamma, the initial volume fraction of the liquid bridge CAPVOL as well as the contact angle CAPANG

between the liquid bridge and the sphere, which is given in radians. The idea of the liquid bridge is shown in Figure 3a) where the volume V_{LB} of the liquid bridge is given in blue and the angle $CAPANG$ in red. In LS-DYNA, the volume of the liquid bridge is assumed to be $CAPVOL$ times one tenth of the average volume of the spheres in contact yielding

$$V_{LB} = \frac{4}{3}\pi (r_1^3 + r_2^3) \frac{1}{10} CAPVOL . \quad (7)$$

Moreover, the critical rupture distance d_{crit} of the liquid bridge is assumed to be a function of its volume V_{LB} as well as $CAPANG$ given in radians yielding

$$d_{crit} = \left(1 + \frac{CAPANG}{2}\right) \sqrt[3]{V_{LB}} . \quad (8)$$

An illustration of the critical rupture distance (8) is given in Figure 3b).

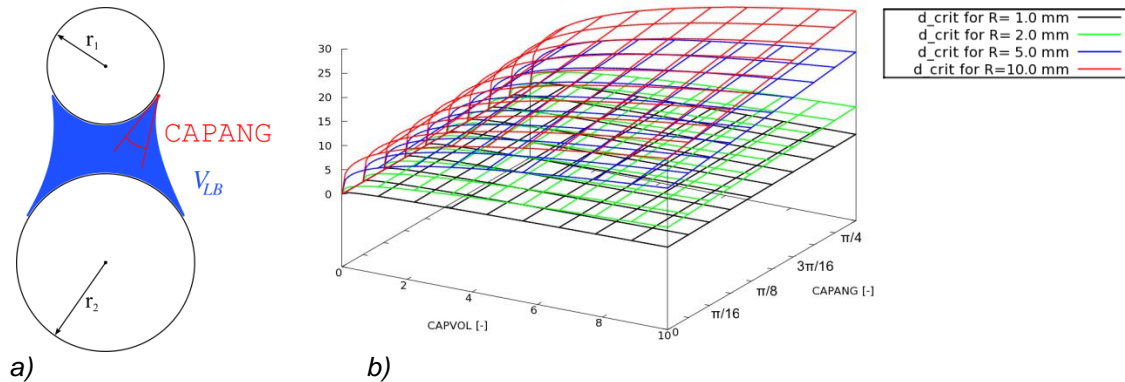


Fig 3: a) Liquid bridge volume V_{LB} and capillary angle $CAPANG$ given in radians between two wet particles and b) dependence of the critical rupture distance d_{crit} on $CAPVOL$ and $CAPANG$.

Following Rabinovich et al. [3], the capillary force can be given by

$$F_n = \frac{\overbrace{2\pi \Gamma \bar{r} \cos(CAPANG)}^{\text{Case I: } d_{int} \leq 0}}{\underbrace{1 + \frac{d_{int}}{d_{sp/sp}}}_{\text{Case II: } 0 < d_{int} \leq d_{crit}}} - 2\pi \Gamma \bar{r} \cos(CAPANG) \quad \text{with} \quad \bar{r} = \frac{2r_1 r_2}{r_1 + r_2} \quad (9)$$

$$d_{sp/sp} = d_{int} + \sqrt{d_{int}^2 + 2 \frac{V_{LB}}{\pi \bar{r}}}$$

Herein, two cases are distinguished, i. e., case I and II, which correspond to a state of mechanical contact and a state without mechanical contact, respectively.

2.3 Particle-Structure Interaction

The particle-structure interaction can be realized using either the classical node-to-surface contact definitions like `*CONTACT_AUTOMATIC_NODES_TO_SURFACE` or the newly implemented routine `*DEFINE_DE_TO_SURFACE_COUPLING`, which was especially designed for the DEM. The difference of the two contact definitions lies in the application of the friction force on the particle as is shown in Figure 4. Herein, the nodes-to-surface contact treats the spherical particle as a mass point, where the friction force is applied to the centroid of the particle without influencing the rotation of the sphere. In contrast, the latter contact definition applies the friction force at the perimeter of the particle, thereby accounting for a moment that is induced on the particle.

The only benefit of the classical nodes-to-surface contacts is the possibility to define a dynamic coefficient of friction besides the static coefficient of friction. However, due to the simplified application of friction forces in the classical nodes-to-surface contacts, it is recommended to use the new contact formulation when setting up simulations.

*DEFINE_DE_TO_SURFACE_COUPLING								
\$#	1	2	3	4	5	6	7	8
\$#	SLAVE	MASTER	STYPE	MTYPE				
\$#	42	1	3	1				
\$#	FricS	FricD	DAMP	BSORT	LCVx	LCVy	LCVz	
	0.5	0.01	0.2	100	0	0	0	

Herein, the spherical particles are always defined as the slave side of the contact using either the ID of a node set, a node, a part set or a part via `STYPE = 0,1,2` or `3`, respectively. The master side can be either given by an ID of a part set or a part using `MTYPE = 0` or `1`, respectively, and may be comprised of deformable finite-element structures (shells or solids) with any kind of material behavior as well as rigid structures, which are defined using `*MAT_RIGID`.

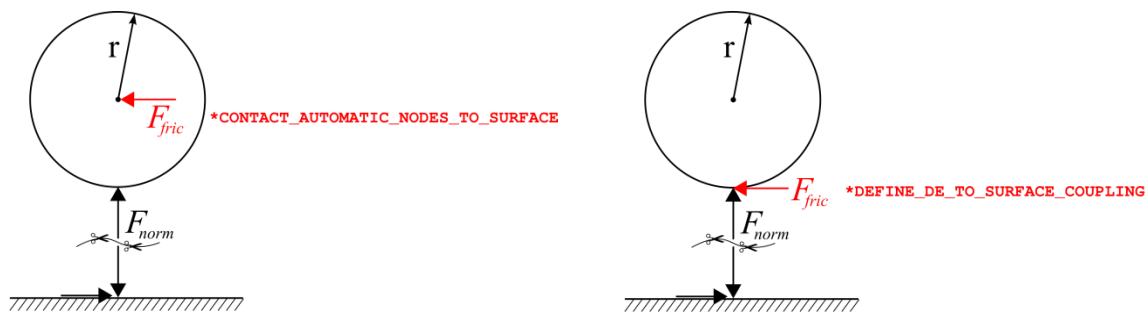


Fig 4: Application of the friction force during particle-structure interaction for a) nodes-to-surface contacts and b) for the newly implemented contact definition for `*ELEMENT_DISCRETE_SPHERE`.

Moreover, as the spherical particles may roll on a surface, there is also the possibility to account for a rolling resistance using the parameter `FricD`. If wet particles are defined, a similar attracting capillary force as given in (9) is applied between the particles and the surface, see Rabinovich et al. [3] for further information. Note that the damping coefficient `DAMP` determines if the collision is fully elastic or fully “plastic” using values of `DAMP` between zero and unity, respectively. Another feature, which is useful when investigating bulk flow analysis, is the possibility to define the velocity of a transportation belt via `LCVxyz` yielding a transport of particles that are in contact with the respective master surfaces. The default number of 100 cycles before an update of the particle neighborhood list (i. e. bucket search) is performed can be altered via `BSORT` in cases, where particles “explode” during the simulation.

Finally, if the structure that comes into contact with the particles consists of beams rather than surfaces, the contact definition `*DEFINE_DE_TO_BEAM_COUPLING` may be used, which follows the same logic as the surface coupling.

Other relevant cards to set up DEM simulations are `*DEFINE_DE_ACTIVE_REGION` as well as `*DEFINE_DE_INJECTION`, which are important to reduce numerical cost during bulk flow analysis. Herein, the first card defines a limiting region using the definition of a box, where the particles are included in the neighborhood lists for potential contact with other objects. The latter card introduces a particle source that generates particles via a mass flow rate through a rectangular plane with pre-defined minimal and maximal radii as well as an initial velocity.

2.4 Extension to Bonded Particles

The above defined loose spherical particles may also be bonded with the card `*DEFINE_DE_BOND`, which is used to simulate the mechanical behavior of an elastic solid as well as brittle fracture analysis. Herein, all spherical particles are automatically linked to their neighboring particles using bonds which represent the complete mechanical behavior of solid mechanics, cf. Figure 5.

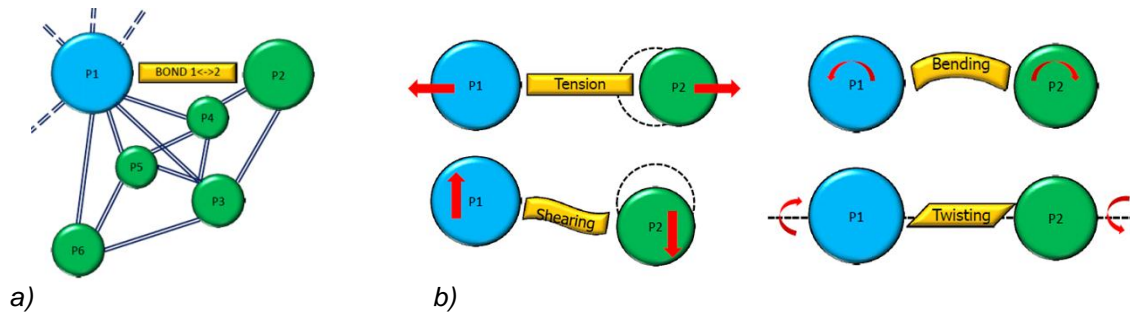


Fig 5: a) Schematic drawing of the possible bonding of particle P1 to its neighbors P2 to P6 and b) possible force and moment transmission modes (i. e. stretching, shearing, bending, twisting) between two bonded particles.

In particular, the mechanical behavior of the bonds between the particles can either be prescribed manually or can be computed internally by LS-DYNA in an automated fashion, which is based on the material constants given in ***MAT_ELASTIC**. The manual definition can be achieved using bond form 1 (BDFORM = 1) yielding

```

*DEFINE_DE_BOND
$#-----1-----2-----3-----4-----5-----6-----7-----8
$#      SID      STYPE      BDFORM      DIM
$#      42       0         1         3
$#      PBN      PBS      PBN_S      PBS_S      SFA      ALPHA      MAXGAP
$#      1.0     1.0     0.285     0.013     1.0     0.2     1.0E-4

```

Herein, SID is the node set ID of the particles to be bonded (STYPE = 0) and DIM = 2 or 3 defines plane stress problems or full 3-d problems, respectively. The parallel (normal) and shear stiffness of the created bonds can be prescribed using the parameters PBN and PBS, respectively. Subsequently, PBN_S and PBS_S define the maximum normal/shear stress at which the bonds rupture. Note that values of zero define infinite maximum normal/shear stresses, such that the bonds never rupture. Moreover, a bond radius multiplier can be prescribed using SFA as well as a damping value using ALPHA. Finally, the maximum gap between two bonded particles can be prescribed via MAXGAP. This is either a multiplier of the smallest radius of the two spheres, i.e. $\text{MAXGAP} * \min(r_1, r_2)$, or an absolute value for the gap, depending on MAXGAP being greater or smaller than zero, respectively.

If BDFORM = 2 is chosen, the mechanical bond characteristics are automatically computed by LS-DYNA such that the overall behavior of the bonded particles is equivalent to a linear-elastic material.

```

*DEFINE_DE_BOND
$#-----1-----2-----3-----4-----5-----6-----7-----8
$#      SID      STYPE      BDFORM      DIM
$#      42       0         2         3
$#      PBK_SF   PBS_SF   FENRGK   FENRGS   BONDR   ALPHA
$#      1.0     1.0     0.285   0.013   3.75   0.0
$#      PRECRK  CKTYPE
$#      12     1

```

To allow for a manual interaction, the automatically computed values for the volumetric and shear stiffness of the bond may be scaled using PBK_SF and PBS_SF, respectively. As BDFORM = 2 is especially designed to perform fracture analysis of brittle materials, the user has the possibility to define fracture energy release rates for volumetric and shear deformations via FENRGK and FENRGS, respectively, cf. Han et al. [2]. Again, a value of zero prescribes infinite fracture energy release rates and thus, unbreakable bonds. Note that the breakage of single bonds can be interpreted as micro cracks that eventually evolve to macro cracks. Moreover, the amount of neighboring particles that are bonded is controlled via BONDR, which is the absolute search radius. Thus, BONDR should be greater than $|\mathbf{x}_1 - \mathbf{x}_2|$, otherwise the spheres in Figure 1a) will not be bonded.

Defining a pre-crack through the bonded spherical particles is straight forward. Herein, the user needs to model the 3-d surface of the pre-crack using shell elements, where PRECRK is the ID of the shell's part set or part using CKTYPE = 0 or 1.

Finally, one also has the possibility to constrain particles to a surface defined by finite elements using the ***CONTACT_CONSTRAINT_NODES_TO_SURFACE** card.

3 Generation of Spherical Particles using LS-PrePost

If no particle source is used in LS-DYNA, every simulation using the DEM requires an initial set of spherical particles that needs to be generated just like a finite-element mesh for classical finite-element analysis. Herein, LS-PrePost® V4.1 can be used to generate an initial particle set using its new built-in sphere packing engine, cf. Han et al. [2]. The sphere generation is possible with user defined but constant sphere radii in single- as well as double-connected volumes, which need to be defined using 3- or 4-noded shell elements with consistent surface normals, cf. Fig. 6.

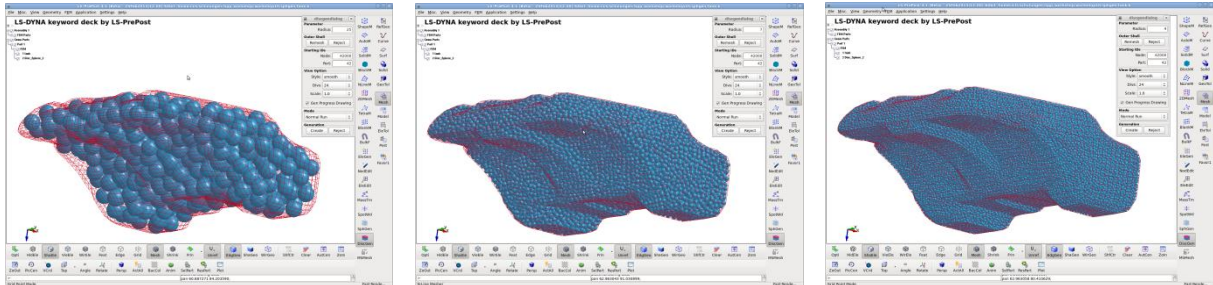


Fig. 6: Sphere packing of a complex geometry using three different but constant sphere radii.

To successfully generate the particles, the user has to enter the *discgen* dialog under *Mesh/DiscGen*. After the bounding surface mesh of the object which should be packed is selected with a mouse click, the user has to enter the desired sphere radius. Thereafter, it is essential that the surface is re-meshed by clicking on *Remesh* as indicated in Figure 7.

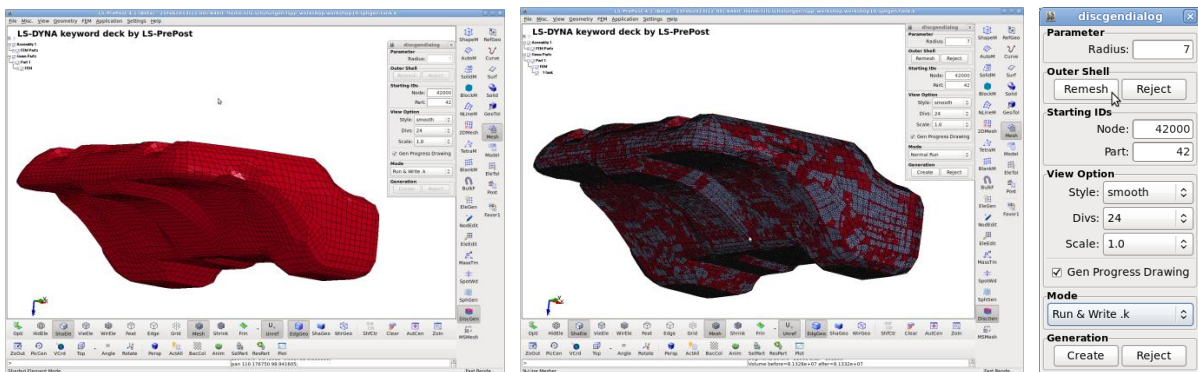


Fig. 7: Workflow of the sphere packing engine in LS-PrePost 4.1.

4 Applications for Loose Particles

4.1 Granular Flow

An important application for the DEM are granular flows which exhibit a fluid-like behavior for the regions that are in motion and a solid-like behavior for regions at rest. To get an impression on the influence of the parameters in **CONTROL_DISCRETE_ELEMENT*, i. e., density, friction and liquid surface tension for particle-particle interaction, as well as **DEFINE_DE_TO_SURFACE_COUPLING* with the friction coefficients for particle-structure interaction, a simple gravity-driven flow through a funnel is presented with varying parameters, viz.:

	1	2	3	4	5
RHO	0.80E-6	2.63E-6	2.63E-6	2.63E-6	1.0E-6
P-P Fric	0.57	0.57	0.57	0.10	0.00
P-P FricR	0.10	0.10	0.01	0.01	0.00
P-W FricS	0.27	0.30	0.30	0.10	0.01
P-W FricD	0.01	0.01	0.01	0.01	0.00
CAP	0	0	1	1	1
Gamma	0.00	0.00	7.20E-8	2.00E-6	7.2E-8
\$---- foamed clay ----- dry sand ----- wet sand --- fresh concrete ----- "water"					

The unit system is kg, mm, ms, kN and GPa and the simulation results of the 5 different parameter settings can be seen in Figure 8.

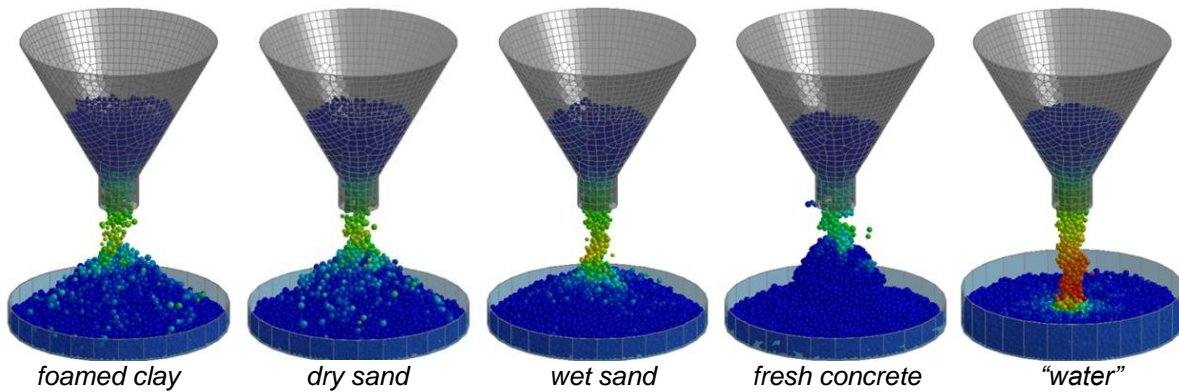


Fig 8: Parameter study to investigate the flow behavior of different dry and wet granular materials.

Another application addresses a hopper flow simulation to investigate undesirable particle deposits or segregation effects inside a silo, see Figure 9 for simulation results.

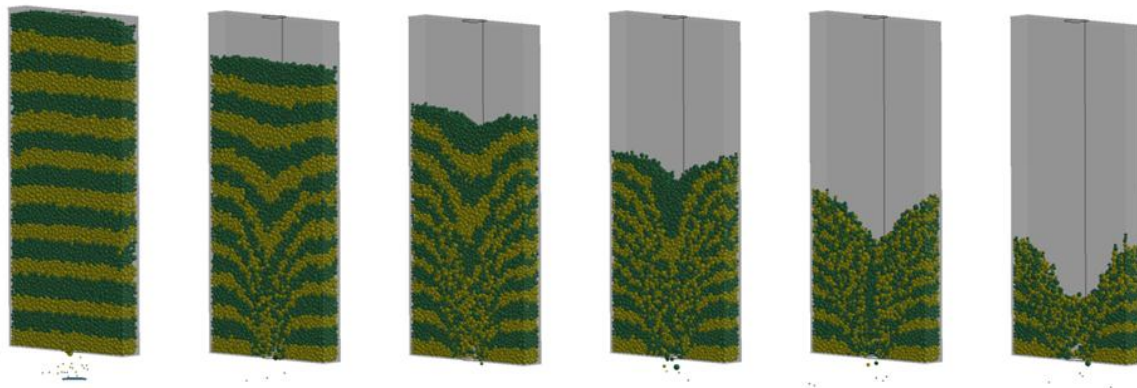


Fig 9: Hopper flow simulation to investigate the flow pattern inside the silo.

4.2 Bulk Flow

A typical example for bulk flow analysis is a conveyor belt, which was simulated with the definition of an active region `*DEFINE_DE_ACTIVE_REGION` to release particles out of interest from the contact search algorithm as well as a particle source via `*DEFINE_DE_INJECTION`.

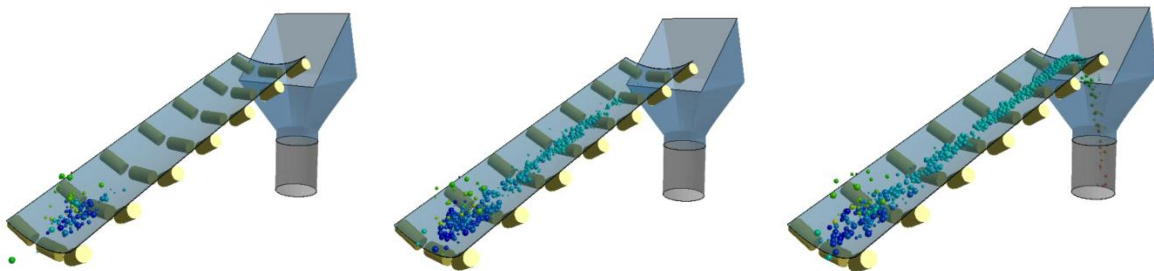


Fig 10: Example of a conveyor belt. The simulation was carried out with a particle source and a deformable belt made of fabric using a transport velocity LCV_{xyz} for the spherical particles.

4.3 Mixing

Another field of application for granular materials addresses mixing processes in a drum mixer. Herein, the granular medium is being transported at the surface of the drum, either via pure friction or by using little notches. Depending on the geometry of the drum itself and the location of its rotational axis, the mixing is more or less efficient. A relatively inefficient mixing process is shown in Figure 11, where two different kinds of spherical particles are supposed to be mixed.

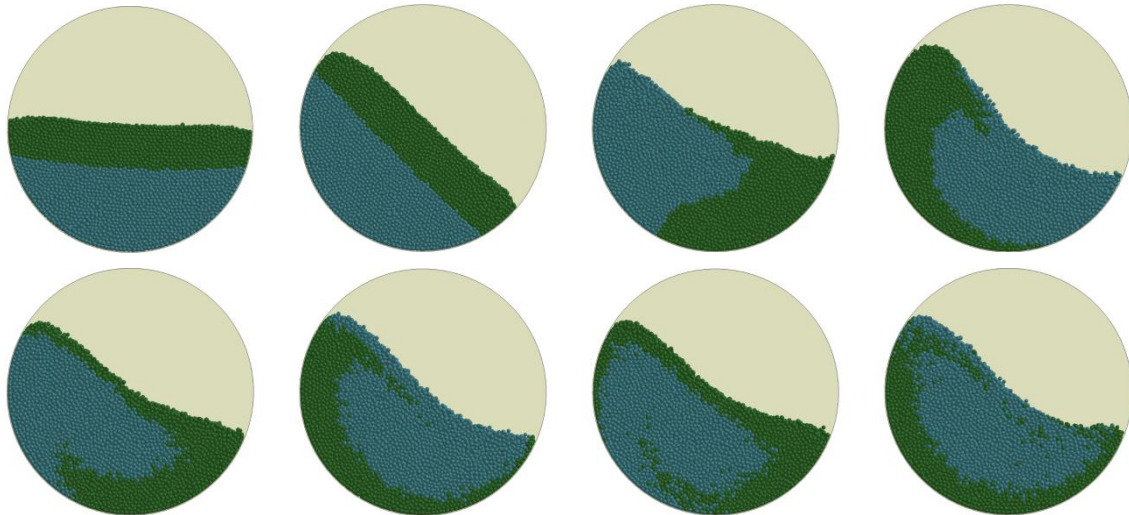


Fig 11: Simulation of a drum mixer containing particles with different densities to investigate the mixing behavior. Foamed clay particles are represented in green, while sand is shown in blue.

4.4 Filling

After the transportation and processing of granular media, there is often the desire to fill the goods in handy packages for sale. During the filling process itself, a segregation of the mixed particles may occur, which can also be investigated using the DEM. Figure 12 shows an example where particles are injected into a thin bag made of fabric, while Figure 13 shows this filling process for 3 different kinds of granular media, i.e. dry sand, wet sand and fresh concrete using the parameters from above. It can be clearly seen, how the capillary forces influence the flow pattern inside the bag.

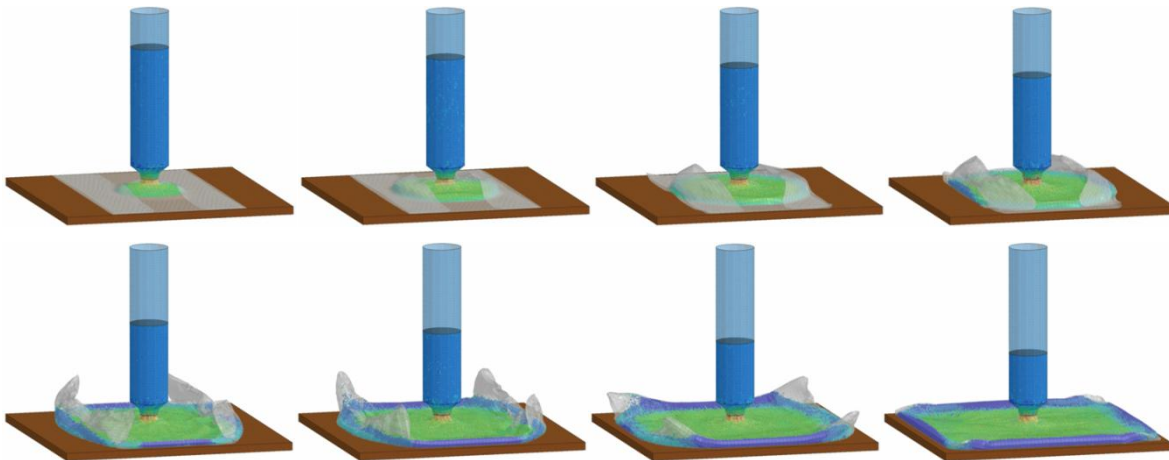


Fig 12: Bag filling simulation of particles being injected into a thin bag made of fabric.

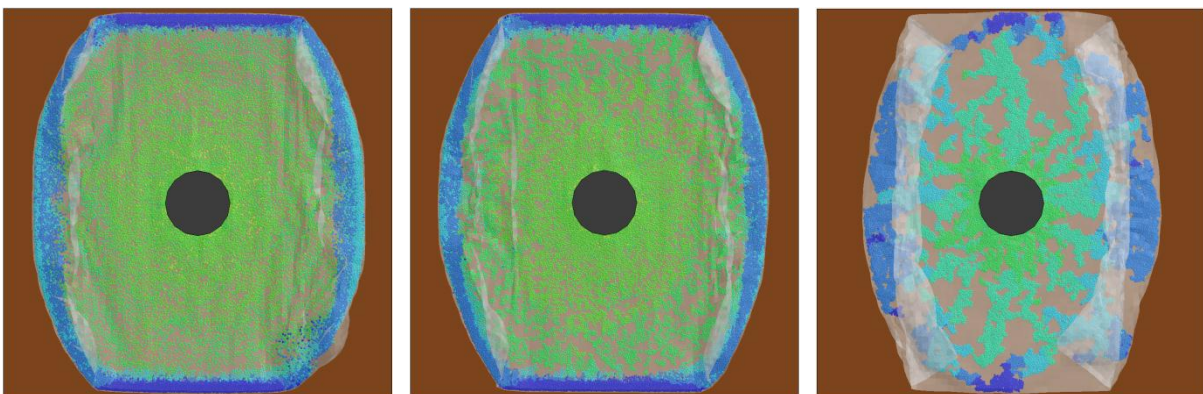


Fig 13: Influence of the liquid bridge on the filling behavior for dry sand, wet sand and fresh concrete.

5 Applications for Bonded Particles

5.1 Linear-Elastic Analysis

Figure 14 shows a benchmark for the automatically created bonds ($BDFORM = 2$) to reproduce linear-elastic material behavior using the example of a beam on two supports under gravity loading with exploitation of the symmetry conditions for different discretizations.

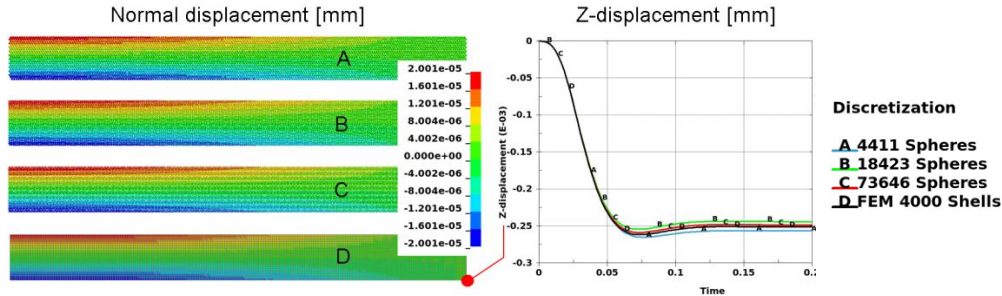


Fig 14: Beam on two supports under gravity loading for different discretizations of bonded particles.

5.2 Brittle Fracture Analysis

Using the automatically created bonds in LS-DYNA enables the user to investigate applications like rock crushing or blasting and failure of concrete or any other brittle material, see Figure 15 and 16.

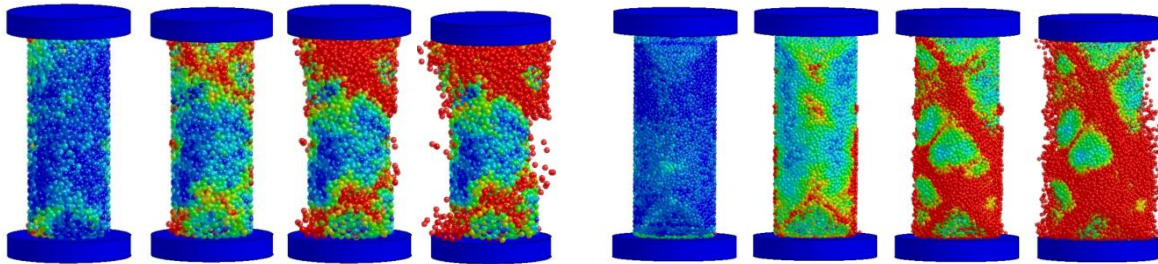


Fig 15: Brittle fracture analysis of a concrete specimen ($h = 100$ mm, $r = 20$ mm) during impact loading (1 mm/ms) using particles with radii of 1.5 mm and 1.0 mm. Blue colors indicate fully functional bonds to the next three neighboring particles, while red indicates fully de-bonded particles.

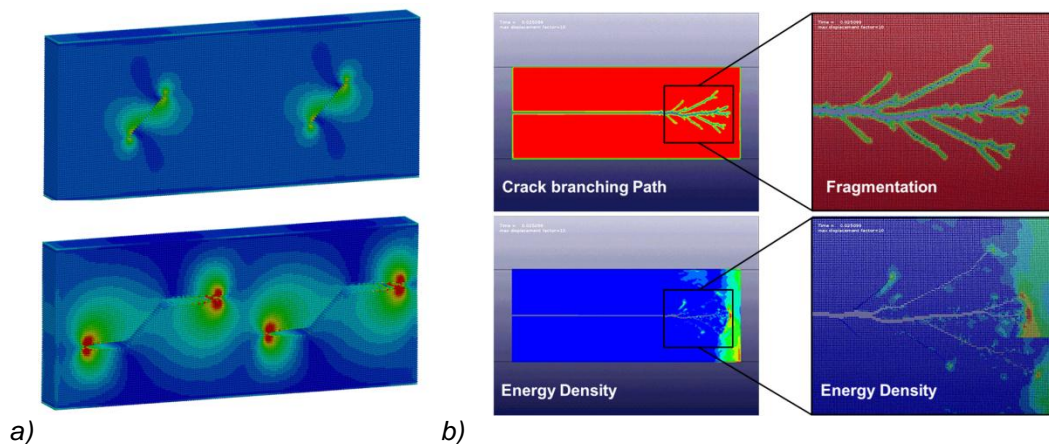


Fig 16: a) Fracture analysis of a pre-cracked glass specimen that is being pulled apart and b) crack fragmentation of a similar glass specimen which is pre-notched on the left side.

6 Literature

- [1] Cundall, P. A. and Strack, O. D. L.: A discrete numerical model for granular assemblies. *Geotechnique* **29** (1979), 47–65
- [2] Han, Z.; Teng, H.; Wang, J.: Computer Generation of Sphere Packing for Discrete Element Analysis in LS-DYNA. *Proceedings of the 12th International LS-DYNA Conference*, Detroit, 2012
- [3] Rabinovich, Y. I.; Esayanur, M. S.; Moudgil, B. M.: Capillary forces between two spheres with a fixed volume liquid bridge: theory and experiment. *Langmuir* **21** (2005), 10992-10997.